ISSN No: -2456-2165 https://doi.org/10.38124/ijisrt/26mar2065

Analysis of RONS Emission Characteristics and Energy Efficiency in Atmospheric DBD Plasma: A Study on Flow Rate Influence toward Excitation Population Distribution

William Arthur Leo[1,3]; Muhammad Nur[2,3*]; Asep Yoyo Wardaya[2]; Eko Yulianto[3]

[1]Magister of Physics, Physics Department, Diponegoro University, Tembalang Campus, Semarang, Indonesia, 50275
[2]Physics Department, Diponegoro University, Tembalang Campus, Semarang, Indonesia, 50275
[3]Center for Plasma Research, Diponegoro University, Integrated laboratory, Tembalang Campus, Semarang Indonesia, 50275

Corresponding Author: Muhammad Nur[*]

Publication Date: 2026/04/11

Abstract: The optimization of operational parameters in Dielectric Barrier Discharge (DBD) plasma technology was highly crucial for generating intensive active species while maintaining efficient energy consumption. This study aimed to analyze the influence of ambient air flow rates on the excitation populations of Reactive Oxygen and Nitrogen Species (RONS) and energy efficiency (EE) through the utilization of Optical Emission Spectroscopy (OES) instruments. Flow rate variations were administered within a range of 2 LPM to 10 LPM. The OES characterization results confirmed the presence of hydroxyl (OH) radicals, the nitrogen (N_2) second positive system, and atomic oxygen (O). The findings demonstrated that an increase in the flow rate induced a significant reduction in the emission intensities of all identified active species. Physically, this phenomenon was governed by the transition of ion mobility from a kinetic control regime to a convective control regime, which shortened the residence time of the species within the discharge zone. The highest Specific Energy Input (SEI) and optimal energy efficiency were identified at the minimum flow rate 2 LPM, where the energy density was capable of triggering maximum ionization prior to the dominance of gas drag forces and quenching phenomena. his study provided critical parameters for the design of efficient ambient air DBD plasma reactors intended for pollutant remediation and energy conversion applications.

Keywords: *Energy Efficiency, Flow Rate Ion Mobility, Quenching, Optical Emission Spectroscopy, Specific Energy Input.*

How to Cite: William Arthur Leo; Muhammad Nur; Asep Yoyo Wardaya; Eko Yulianto (2026) Analysis of RONS Emission Characteristics and Energy Efficiency in Atmospheric DBD Plasma: A Study on Flow Rate Influence toward Excitation Population Distribution. *International Journal of Innovative Science and Research Technology,* 11(3), 3837-3847. https://doi.org/10.38124/ijisrt/26mar2065

I. INTRODUCTION

Non-thermal plasma technology, particularly Dielectric Barrier Discharge (DBD), is extensively utilized across various industrial applications due to its capacity for molecular dissociation and the generation of Reactive Oxygen and Nitrogen Species (RONS)[1,2]. The operation of DBD reactors is performed with a strict emphasis on energy efficiency to facilitate remediation processes and energy conversion.[3,4]. Research indicates that the effectiveness of DBD in generating hydroxyl radicals (OH), excited nitrogen (N2), and atomic oxygen (O) is highly contingent upon reactor design and energy management for the degradation of persistent pharmaceutical pollutants[3,5]. Furthermore, the integration of dielectric materials and the optimization of electrode configurations currently represent a primary focus for enhancing plasma emission stability. These strategies are implemented to maximize the production yield of reactive species within both humid and ambient air environments [4,6,7].

The utilization of Printed Circuit Boards (PCB) as a substrate for reactor design is developed to facilitate assembly and the integration of sensors for more precise control over plasma physical parameters [8,9]. Other studies emphasize the significance of the dielectric-guided discharge

ISSN No: -2456-2165 https://doi.org/10.38124/ijisrt/26mar2065

mechanism within microchannels to maintain ionization sustainability, which is influenced by the interaction between the electric field and the gas flow [10]. This phenomenon is considered highly crucial when the system operates at varying flow rates, as it determines the transport regime of active species from the discharge zone to the reaction target.

However, reactors are frequently constrained by power consumption that is disproportionate to the production of active species. In plasma reactor systems, the Specific Energy Input (SEI) parameter serves as a primary indicator for determining Energy Efficiency (EE). While high power intake is capable of enhancing electron density, it is not consistently proportional to species production if the residence time is not optimized [1,11,12]. In the absence of flow rate optimization, energy is dissipated as heat, which triggers thermal quenching and reduces the probability of effective collisions between energetic electrons and gas molecules [13,14,15].

The flow rate plays a pivotal role in regulating dynamics and particle kinetics within the reactor through the modulation of residence time and quenching mechanisms. In high-pressure surface DBD systems, an increase in the flow rate from 0.5 to 5 LPM reduces the plasma area and the quantity of streamers, however, it enhances high power conversion due to the improvement in effective contact time [8,15,16]. Studies on hybrid DBD utilizing humid air demonstrate that low flow rates of less than 1 LPM generate a high SEI exceeding 150 J/L for nitrogen-based species, such as N2O5 and HNO3, which subsequently diminish at flow rates surpassing 5 LPM [5]. OES characterization confirms a reduction in OH and O emission intensities by up to 60% as the flow rate is increased, signifying a decrease in RONS concentration caused by quenching from O2 and H2O molecules [11,15,16,17]. In fluidized-bed plasma reactors, an optimal flow rate of 0.10 m/s is requiered to establish uniform fluidization and efficient power distribution, thereby mitigating RONS overproduction [11].

Furthermore, variations in gas flow rates trigger a fundamental transition in the ion transport modes within the reactor. At low flow rates, the system is primarily governed by electric field influences. However, as the flow rate increases, the system transitions toward a more dominant convective transport regime [18]. This transition induces a reduction in the intensity of active species due to shortened interaction times and the presence of selective hindrance resulting from size-exclusion effects on molecular mobility within the plasma [19,20].

Electrical characterization demonstrates that flow rates exceeding 3 LPM reduce the SEI per gas volume by up to 40% and enhance the EE by a factor of three compared to static systems [3,5]. However, the majority of existing studies employ inert gases, such as Argon (Ar) and Nitrogen (N2) to ensure discharge stability [1,7,17,21]. conversely, ambient air generates complex RONS chemistry due to the 21% presence of O2 content and variable humidity H2O, thereby rendering the system more sensitive to flow rate fluctuations [5,22]. During molecular dissociation and recombination reactions, Optical Emission Spectroscopy (OES) enables real-time particle detection for the identification of reactive species. Characteristic emission peaks of RONS, specifically (309 nm), atomic O (777 nm), and N2 (337 nm), are captured via OES Fluctuations in emission intensity reflect the RONS concentration and electron density within the plasma [16,17,18,23,24]. Studies on triple-electrode RF configurations indicate a transition from filamentary to glow modes at frequencies exceeding 10 kHz, which is characterized by the homogenization of N2 emissions and an enhancement in discharge stability [18,24].

Although OES is extensively utilized for RONS characterization, a systematic study examining the influence of ambient air flow rates on the reduction of RONS intensity has not yet been conducted. Through real-time analysis, the OES emission peaks of OH, O, and N2 are identified in conjunction with the enhancement of energy efficiency within DBD reactors [16,18,24]. There remains a deficiency of quantitative data regarding the correlations between flow rate, emission intensity, RONS concentration, and EE under ambient air conditions.

This study aims to investigate the influence of ambient air flow rates on the reduction of RONS intensity. Characterization is performed in real-time through the observation of OES emission intensities within the DBD plasma reactor. The focus of this research is directed toward plasma characterization utilizing OES as the primary diagnostic tool. This research is expected to provide fundamental data for the development of controlled, energy-efficient, and scalable ambient air-based DBD systems.

II. RESEARCH METHODS

Ambient air was utilized as the primary research sample throughout this study. The Dielectric Barrier Discharge (DBD) reactor was constructed from Pyrex glass, where aluminum foil was adhered to the external surface and an aluminum mesh was integrated into the interior to function as electrodes. The reactor featured an internal diameter of 4.5 cm, a wall thickness of 0.2 cm, and a total length of 40 cm. The reactor assembly was encased in a polyvinyl chloride (PVC) pipe and subsequently interfaced with a power source, a helium gas cylinder, and a flow meter, as illustrated in Figure 1. Upon activation of the reactor, a uniform discharge was generated along the length of the tube, facilitated by the mesh-type winding configuration attached to both the outer and inner diameters of the Pyrex glass.

ISSN No: -2456-2165 https://doi.org/10.38124/ijisrt/26mar2065

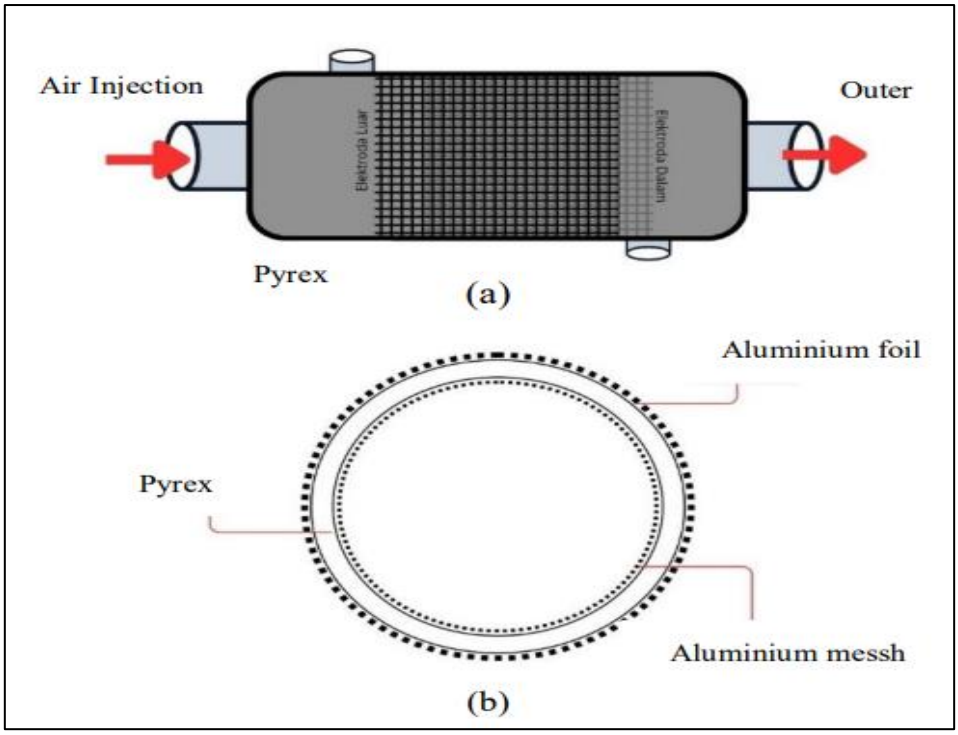

Fig 1 The DDBD Reactor Uses Mesh Electrodes (a) Side view; (b) Front View.

The electrodes used have an aluminum mesh configuration that covers the outside and inside of the reactor Pyrex tube. Pure oxygen was used as a feed-gas source. The volumetric flow rate of the oxygen gas into the generator was set to be 0.2 L/min, 0.4 L/min, 0.6 L/min and 0.8 L/min, while the voltage discharge applied to the DDBD was 3 kV. The two electrodes are connected to a pulsed AC high voltage source which functions to supply high voltage to the reactor with voltage variations ranging from 0 kV to 10 kV Volts and a frequency of 60 Hz (produced by Dipo Technology, Indonesia) as a source of potential, while the output voltage waveform across the two electrodes of the DDBD plasma was measured using a high voltage probe (AC/DC max voltage 40 kV, EC 1010, EnG1010 Taiwan), respectively, and an oscilloscope (GOS-653 50 MHz). The output current discharge was measured by an analog multimeter (Sanwa YX361TR, China).

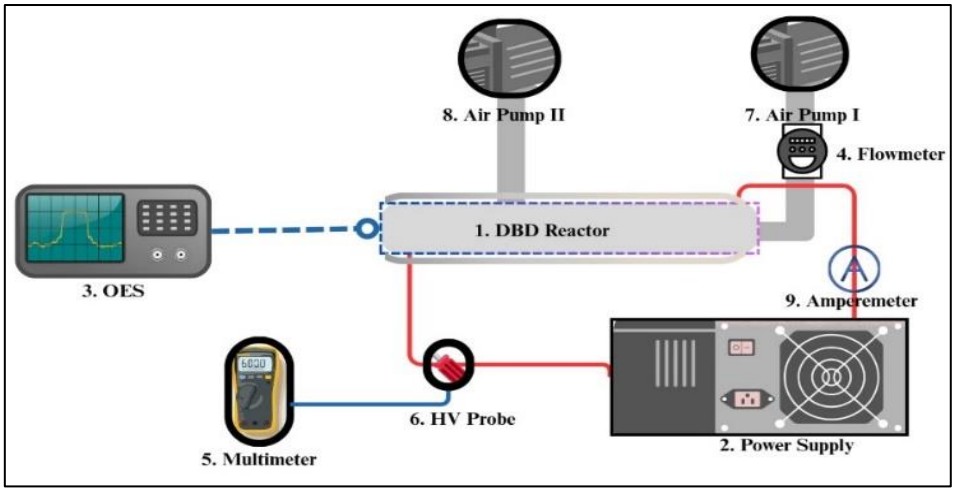

Fig 2 Schematic Diagram of the Experimental Setup for Investigating the Influence of Flow Rate on RONS Excitation Populations

The data acquisition procedure was initiated with a preparation stage and instrument characterization to ensure the validity of the measurement results. The Dielectric Barrier Discharge (DBD) reactor system (1) was interfaced with an AC high-voltage power supply (2), while the air supply system from pump 1 (7) was ensured to be hermetically sealed to prevent any leakage. The AC high voltage was monitored utilizing an HV Probe (6) to attenuate the voltage values at a 1:1000 ratio, thereby enabling precise measurements via the Multimeter (5) and Ammeter (9). Subsequently, plasma discharge was generated within the reactor to induce the dissociation of ambient air, which was subsequently identified using OES (3) to analyze the RONS constituents.

ISSN No: -2456-2165 https://doi.org/10.38124/ijisrt/26mar2065

Following the completion of the preparation stage, the data collection process was commenced by varying the current against the voltage (I-V). The I-V variations were performed to determine the ion mobility, which generally represents the particle kinetics within the reactor during the operation of the plasma system. In this context, ion mobility was influenced by distance, whereas the gas flow rate exerted a highly significant impact [18]. Mathematically, the ion mobility was determined using the following Equation (2):

$$I_s = \frac{2\mu\varepsilon_0\varepsilon_r N}{d} V^2 \quad (1)$$

$$\mu = \frac{I_s d}{2\varepsilon_0\varepsilon_r N V^2} \quad (2)$$

Where μ represents the ion mobility (m^2/Vs), I_s denotes the electrical current (Ampere), V signifies the applied voltage (Volt), d refers to the inter-electrode distance (meter), N indicates the number of electrode points, ε_0 is the vacuum permittivity $8{,}854 \times 10^{-12}\,(\mathrm{F/m})$, and ε_r represents the dielectric constant of the Pyrex ceramic medium, which is 4.6. The ambient air flow rate was utilized as the primary independent variable. Air was channeled into the reactor via a flow meter, starting from a static condition and progressing through 2, 4, 6, 8, and 10 LPM. At each flow rate variation point, voltage increments were applied starting from 0 kV until the reactor reached a maximum operating voltage of 15 kV. Data acquisition was performed in real-time and simultaneously between the optical and electrical diagnostics at each flow rate interval.

The plasma emission spectra were continuously recorded by the OES, with the observational focus directed toward the peaks of dominant species, such as hydroxyl radicals (OH), molecular nitrogen (N2), and atomic oxygen (O). These intensity data were utilized to evaluate the excitation population of RONS. Variations in flow rate and voltage were implemented to identify particle populations during the increments of both flow rate and applied voltage. The entire spectral dataset was subsequently validated to ensure the absence of signal saturation or electromagnetic interference. To guarantee data reliability and precision, the aforementioned procedure was replicated ten times under identical environmental conditions, and the final results were calculated as average values prior to the data analysis stage.

SEI was defined as a critical parameter that determined the effectiveness of molecular excitation processes within the plasma zone. SEI was analyzed as a function of voltage across air flow rate variations of 2, 4, 6, 8, and 10 L/min. The SEI was formulated through Equation (3) [11]:

$$SEI = \frac{P}{Q} \times 60 \quad (3)$$

Where SEI defined as the Specific Energy Input (J/L), P was the discharge power (Watt or J/s), and L is the gas flow rate (LPM).

EE was employed to evaluate the DBD reactor performance based on the intensity of the generated radicals. The EE was expressed using the following Equation (4):

$$EE = \frac{I}{P} \quad (4)$$

In this formula, EE was defined as the energy efficiency (a.u./J), I was the intensity (a.u.), and P was the power (W)[5].

III. RESULT AND DISCUSION

- *Current-Voltage (I-V) Characterization and Ionic Mobility*

Characterization of the current-voltage (I-V) relationship was performed to evaluate the operational stability and ionization efficiency within the Dielectric Barrier Discharge (DBD) reactor. Based on experimental observations, the alterations in current demonstrated a robust dependence on voltage variations within the range of 0 kV to 15 kV. The onset of plasma is characterized by a distinctive shift in the current increment trend, which is illustrated in Figure 4. An increase in current causes electrons to collide with the passing air at higher velocities, thereby accelerating the molecular dissociation process. These electronic collisions subsequently generate ions and excited particles, which are observable as purple visible light, as depicted in Figure 3.

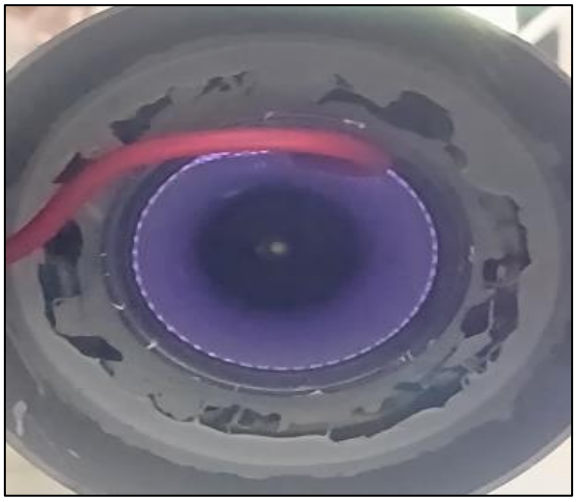

Fig 3 Visible Plasma Discharge Generated Within the Dielectric Barrier Discharge (DBD) Reactor.

Gas flow rate variations at 2, 4, 6, 8, and 10 LPM demonstrated the influence of charge dynamics on the current alterations within the reactor gap. The I-V curves indicate that the utilization of an aluminum mesh electrode, which is adhered to the interior of the Pyrex ceramic barrier, intensifies the local electric field. This intensification accelerated the breakdown conditions, which were successfully achieved at a voltage of 4 kV. This phenomenon

ISSN No: -2456-2165 https://doi.org/10.38124/ijisrt/26mar2065

facilitates the initiation of more homogeneous micro-discharges in comparison to the use of solid cylindrical electrodes, thereby reducing the activation energy required to trigger the ionization of ambient air.

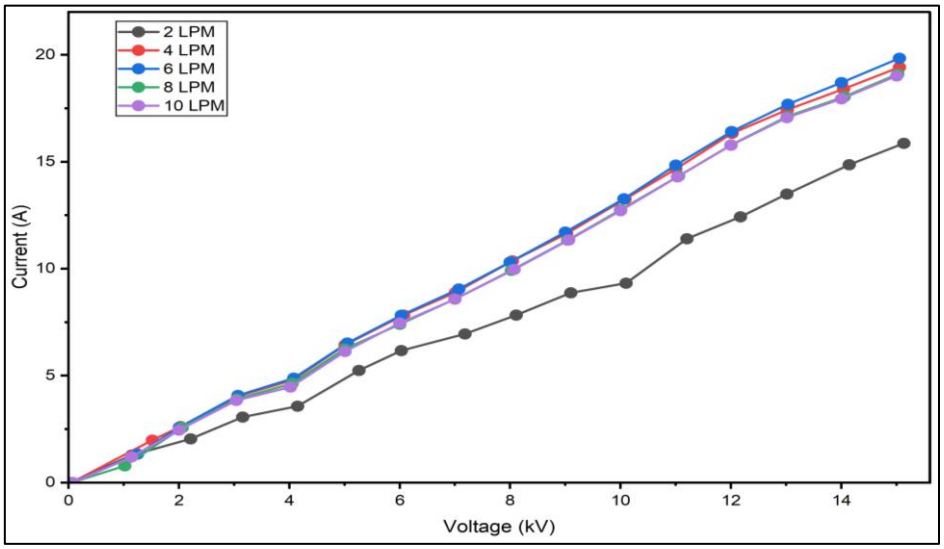

Fig 4 Comparison of Current-Voltage (I-V) Characteristics under Varying Gas Flow Rate Conditions.

Variations in gas flow rates at 2, 4, 6, 8, and 10 LPM demonstrated the influence of charge dynamics on current fluctuations within the reactor gap. The current-voltage curves indicated that the utilization of an aluminum mesh electrode, which was mounted flush against the interior of the Pyrex ceramic barrier, contributed to the enhancement of the local electric field, thereby allowing the breakdown condition to be achieved at a voltage of 4 kV. This phenomenon facilitated the initiation of more homogeneous micro-discharges compared to the use of solid cylindrical electrodes, which subsequently lowered the activation energy required to trigger the ionization of ambient air.

Within the reactor, electron mobility is significantly greater than ion mobility due to the substantial difference in particle mass. Electrons are accelerated by the localized electric field and subsequently collide with the ambient air traversing the discharge gap, which induces molecular dissociation. Particles in the air were dissociated by electron impact, resulting in the generation of ions that continuously propagated along the reactor length [9, 10].

A significant increment in current was observed during the transition from a flow rate of 2 LPM to 4 LPM. This phenomenon is explicable through the concept of ion mobility within the discharge medium. Based on Equation (2) and the obtained experimental results, it was determined that ion mobility was substantially influenced by the gas flow rate. A noteworthy phenomenon is identified, wherein the ion mobility achieves an optimal state as a function of the flow rate, as illustrated in Figure 5.

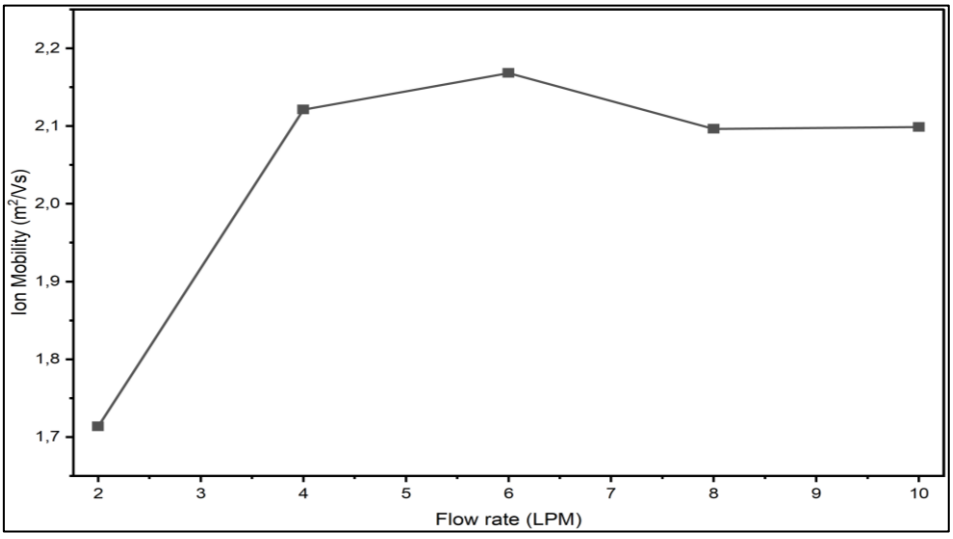

Fig 5 Ion Mobility Alterations as a Function of Gas Flow Rate Variations

ISSN No: -2456-2165 https://doi.org/10.38124/ijisrt/26mar2065

Figure 5 illustrates the phenomenon of ion mobility alterations in response to varying gas flow rates. When the flow rate was increased from 2 LPM to 4 LPM, a significant elevation in ion mobility was observed. This increment is attributed to the gas flow, which facilitates a more uniform charge distribution across the electrode surface. The flow enhances the gas density within the discharge gap, thereby enabling ions to move more fluidly without being significantly impeded by excessive thermal agitation. This current surge indicates that the gas flow assists in distributing charged species more effectively across the dielectric barrier area[9].

Subsequently, the mobility continued to increase at 6 LPM, yet a decline was recorded at 8 LPM. This reduction signifies the occurrence of a quenching effect [1]. At excessively high flow rates within a narrow gap, gas molecules move at higher velocities with increased stochasticity, which elevates the collision probability between ions and neutral molecules before the ions reach the electrode. Consequently, the average velocity or effective mobility of the ions decreases. As the flow rate escalates, neutral gas molecules exhibit rapid movement and turbulence, causing particles to collide more frequently prior to reaching the collecting electrode. This phenomenon reduces the effective ion mobility and subsequently influences the electrical current values measured at the collecting electrode. At 10 LPM, a stable condition was reached, indicating that further increases in the flow rate no longer significantly altered the charge density.

➢ *The Influence of Gas Flow Rate on Excitation Populations*

Figure 3 below shows the ozone concentration as a function of applied voltage for several flowrate variations, namely 0.2 L/min, 0.4 L/min, 0.6 L/min and 0.8 L/min. In this picture it can be seen that when the voltage is increased there is an increase in the ozone concentration. This is because the amount of energy possessed by the particles is getting bigger. The transfer of energy and momentum allows ionization, the dissociation of oxygen molecules when collisions occur. This collision results in the formation of more ozone. To provide conditions for initial medical ozone production, this reactor can produce it with a voltage of 3270 volts, as can be seen in Figure 3.

The spectroscopic results demonstrated the identification of excited particles generated during the plasma discharge within an ambient air medium. Active species were identified using OES to validate the formation of RONS within the plasma zone. The captured emission spectra, which included molecular nitrogen (N2) within the 330–385 nm [3,18], hydroxyl radicals (OH) within the 306–310 nm [3,11], and atomic oxygen (O) at 777.4 nm[1,3], are presented in Figure 6. Furthermore, at a constant flow rate of 10 LPM, voltage variations were applied at 10 kV, 12 kV, and 14 kV.

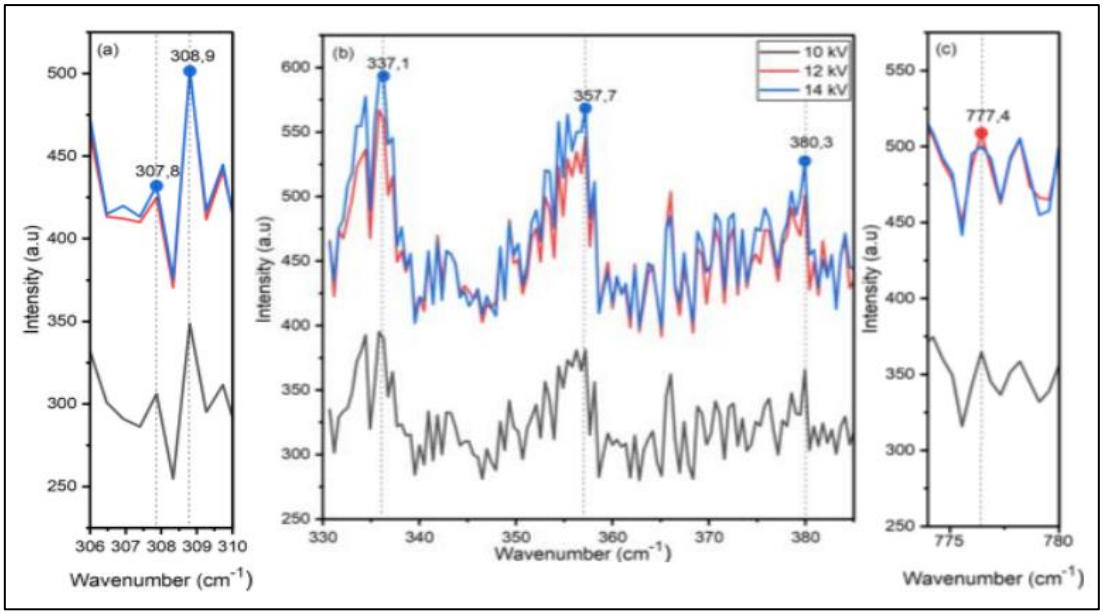

Fig 6 Effect of Voltage Variations on the Excitation Intensities of (a) Hydroxyl Radicals within the 306–310 nm, (b) Nitrogen within the 330–385 nm, and (c) Atomic Oxygen at 777.4 nm Radicals within the Plasma Discharge

Figure 6 (a) illustrates the emission spectrum of hydroxyl radicals, which are generated when ambient air molecules undergo dissociation through direct electron impact or interaction with excited oxygen atoms. These radicals function as potent oxidants within the plasma system, facilitating the degradation of organic pollutants. Figure 6 (b) presents the emission spectrum of excited nitrogen species. The nitrogen peaks represent the most dominant emissions observed in ambient air plasma spectroscopy. The nitrogen bands indicate that electrons possess sufficient energy to promote nitrogen molecules into higher energy levels through inelastic collisions. Figure 6 (c) exhibits a distinct peak at 777.4 nm, signifying the dissociation of oxygen molecules, which plays a pivotal role in the formation of ozone.

A surge in the molecular excitation population was observed when the applied voltage was increased from 10 kV to 12 kV. Visually, this increment signifies an enhancement

ISSN No: -2456-2165 https://doi.org/10.38124/ijisrt/26mar2065

in electron density and the frequency of inelastic collisions, which are effective for the dissociation of ambient air molecules. However, the population intensity remained nearly constant when the voltage was further increased to 14 kV. The population intensity exhibits a quasi-static behavior under these conditions. This phenomenon indicates that molecular excitation generates an accumulation of energy. The energy is converted into photon emissions and subsequently absorbed through thermal quenching mechanisms to drive secondary chemical reactions, such as the synthesis of more abundant molecules like ozone.

Additional spectroscopic analyses were performed to determine the influence of gas flow rate variations on the emission intensity of excited particles within the plasma state. The implementation of flow rate variations at 2, 4, 6, 8, and 10 LPM yielded significant effects on the spectral characteristics, as illustrated in Figure 7.

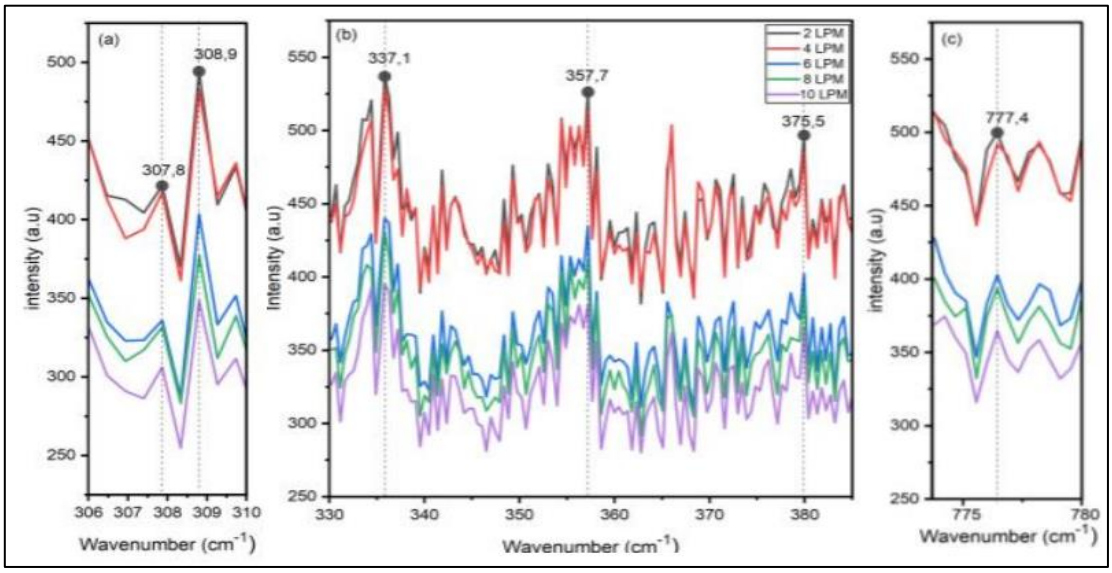

Fig 7 Effect of Flow Rate Variations on the Excitation Intensities of (a) Hydroxyl Radicals within the 306–310 nm, (b) Nitrogen within the 330–385 nm, and (c) Atomic oxygen at 777.4 nm Radicals within the Plasma Discharge.

In general, Figure 7 presents spectroscopic results that deviate from Figure 6 due to the influence of the gas flow rate. The influence of the gas flow rate on the emission population intensities of OH, N2, and O exhibits a transitional pattern. The graph illustrates the particle kinetics within the reactor environment. Within the flow rate range of 2 LPM to 4 LPM, the emission intensity populations of the three radicals appeared stable, with a marginal decline observed. This phenomenon indicates that in the low-flow regime, the gas residence time within the discharge gap is sufficiently long to facilitate the occurrence of molecular excitation. Minor variations in the flow did not drastically alter the population of excited species at the OES sensor interface. As the flow rate was increased from 4 LPM to 6 LPM, a sharp decrease in the population was observed, signifying a transition from reaction kinetics toward convective transport. At 6 LPM, the linear gas velocity begins to surpass the diffusion rate of short-lived radicals, such as OH and atomic O. These species exit the detection zone more rapidly or undergo recombination into stable molecules, such as H2O2 or O3 before photon emission can occur. The significant reduction from 4 LPM to 6 LPM was directly correlated with the peak ion mobility identified during the electrical characterization.

At flow rates ranging from 8 LPM to 10 LPM, the emission intensities once again exhibited a trend toward stabilization. This phase indicates that the system is increasingly approaching the minimum threshold for electron-molecule interaction time. Exceedingly high flow velocities cause the probability of inelastic collisions per unit gas volume to become severely limited. This condition establishes the fundamental relationship between gas residence time and the formation efficiency of reactive species within the DBD reactor. The dynamics of energy transfer at the molecular scale provide an explanation for these observed processes.

A prolonged residence time at low flow rates provides the opportunity for gas molecules to absorb energy from the electric field in a sustained manner [11]. Low flow rates maximize the probability of inelastic collisions, which trigger the dissociation and excitation of species such as OH and N2. Conversely, an increase in the flow rate shortens the residence time of molecules within the discharge zone. The escalation of the flow rate induces a quenching mechanism [6]. Under these conditions, the energy that should be released as photon emission is dissipated through non-radiative collisions with rapidly passing neutral gas molecules. This phenomenon resulted in a reduction of both the OES spectral population intensity and the energy efficiency. The input energy was not optimally utilized for the production of active species, but was instead dissipated as kinetic energy due to the high frequency of quenching collisions before the species could reach a stable state. The reactions occurring during this phenomenon are further elucidated in Table 1.

ISSN No: -2456-2165 https://doi.org/10.38124/ijisrt/26mar2065

Table 1 Proposed Reaction Mechanisms and Pathways for RONS Generation in the DBD System.[1, 13]

Mechanism reaction	Reaction Equations
Electron Impact Excitation	$e + N_2 \rightarrow N_2(C^3\Pi_u) + e$
Radiative De-excitation	$N_2(C^3\Pi_u) \rightarrow N_2(B^3\Pi_g) + hv$
Electron Impact Dissociation	$e + H_2O \rightarrow \cdot OH + H + e$ $N_2 + H_2O \rightarrow N_2 + \cdot OH + H$
Optical Emission (306-310 nm)	$OH(A^2\Sigma^+) \rightarrow OH(X^2\Pi) + hv$
Molecular Dissociation	$e + O_2 \rightarrow O + O + e$ $O(3p^5P) \rightarrow O(s^5S) + hv$
Three-body Recombination	$O + O_2 + M \rightarrow O_3 + M$

The formation of RONS within the DBD reactor involves a series of inelastic electron collisions that trigger molecular dissociation and excitation reactions. Spectroscopically, the Nitrogen emission intensity dominates the spectrum within the 310–380 nm range through the Second Positive System (SPS) mechanism. This process is initiated by high-energy electrons exciting nitrogen molecules to the $C^3\Pi_u$ energy level prior to decaying back to the ground state [6, 11]. Meanwhile, Hydroxyl radicals at a wavelength of 309 nm are generated through the dissociation of water vapor in the ambient air or via energy transfer from metastable nitrogen species [15]. The emergence of the Atomic Oxygen emission peak at 777 nm substantiates the occurrence of oxygen molecule dissociation, which serves as a critical precursor for the formation of molecular oxidants [7].

The emission population intensities of the three species were observed to decrease as the flow rate increased, which resulted in a significantly shorter residence time of the gas molecules within the discharge zone. This reduction limits the probability of sustained excitation occurrences [1, 11]. Quenching mechanisms contribute to this condition, wherein the excitation energy of active species is dissipated through non-radiative collisions with rapidly passing neutral gas molecules rather than being emitted as photons [10]. Consequently, the density of active species measured via OES intensity is reduced, which directly reflects a decline in the energy transfer efficiency from the electric field to the gas particles [15].

- *Energy Efficiency (EE) Analysis*

An increase in the gas flow rate within the DBD system exerts a substantial impact on the dynamics of charged particles and energy efficiency. The elevation of the flow rate enhances the convective velocity of the gas, which drastically shortens the residence time of molecules within the plasma zone. This phenomenon influences ion mobility, as higher flow rates accelerate transportation, thereby limiting the interaction duration between high-energy electrons and primary gas molecules. Consequently, the energy density absorbed per unit volume of gas, formally recognized as SEI, was observed to undergo a significant reduction as the flow rate increased [7, 12].

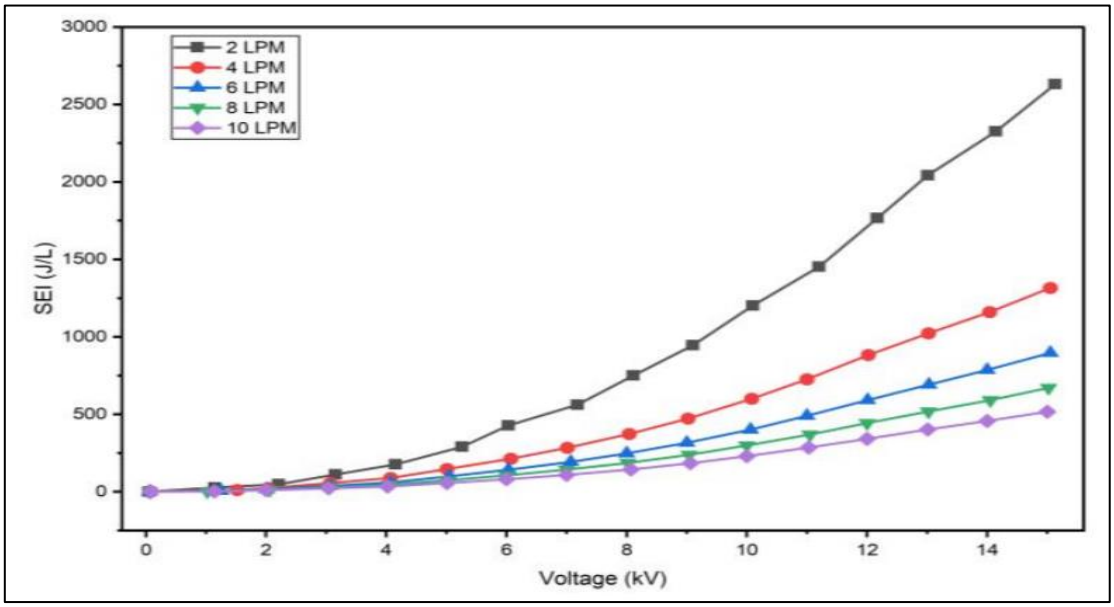

Fig 8 Influence of Applied Voltage on the Specific Energy Input (SEI) Across Various Gas Flow Rate Configurations.

ISSN No: -2456-2165 https://doi.org/10.38124/ijisrt/26mar2065

Overall, the SEI exhibits a linear upward trend in response to the voltage increments across all gas flow rate variations. This indicates that as the voltage increases, a greater magnitude of electrical energy is dissipated into the system, which theoretically triggers the formation of reactive species, such as RONS. At a flow rate of 2 LPM, the generated SEI was recorded at 1202.04 J/L at an applied voltage of 10 kV. However, at a constant voltage of 10 kV, a drastic reduction in the SEI to 229.50 J/L was observed when the flow rate was escalated to 10 LPM. This decrement elucidates the energy dilution phenomenon, wherein gas molecules experience a progressively shorter residence time as the flow velocity is intensified. This phenomenon accounts for the attenuation of OH, O, and N2 radical intensities detected in the OES spectra, as illustrated in Figure 6.

Although the voltage increased the SEI linearly, EE exhibited a decline at higher voltages, which aligned with the principle of power dissipation as the electrical energy was converted into thermal energy rather than chemical energy for radical formation. The performance evaluation of the DBD reactor was contingent upon both the generated radical intensity and the energy efficiency.

Table 2 presents EE values relative to the flow rate variations under an operational voltage of 10 kV. The EE was expressed through the following Equation (4). Based on the obtained data, a declining trend in EE was found as the gas flow rate increased. At a flow rate of 2 LPM, the highest efficiency of 38.20 a.u./W was achieved with a SEI of 1202.04 J/L. Conversely, at a flow rate of 10 LPM, the EE value decreased to 28.98 a.u./W as the SEI value declined to 229.50 J/L.

Table 2 Variations in Energy Efficiency (EE) as a Function of Emission Intensity and Discharge Power Under Different Gas Flow Rates

Flow rate (LPM)	**Power** (Wcm^{-3})	**SEI (J/L)**	**Intensitas (a.u)**			**EE (a.u/W)**
			OH	O	N	
2	40,0	1202,0	494,2	536,8	499,7	38,2
4	39,9	599,8	482,0	528,6	491,8	37,5
6	40,0	400,4	403,5	440,1	402,6	31,1
8	39,8	298,5	377,0	436,6	393,8	30,3
10	38,2	229,5	348,6	396,1	364,7	28,9

The reduction in energy efficiency confirms that while an increase in the flow rate elevates the molecular density, the probability of effective collisions between electrons and gas molecules is simultaneously diminished. The Table illustrates the alterations in SEI between 2 LPM and 6 LPM, which serves to substantiate the previously discussed ion mobility data. The radical production efficiency was significantly hindered as the system entered a more dominant convective transport regime.

The reduction in energy efficiency confirmed that although higher flow rates increased the quantity of molecules traversing the reactor, the probability of effective collisions between electrons and gas molecules was diminished due to the excessively low SEI. The table demonstrated a broad SEI phenomenon between 2 LPM and 6 LPM, which supported the previously discussed ion mobility data, wherein the efficiency of radical production was hindered as the system entered a more dominant convective transport regime.

Although high flow rates may enhance the mass transfer of species such as ozone, a threshold for the degradation of EE is observed. The decline in EE at elevated flow rates occurs because the input energy is no longer optimal to trigger maximal molecular ionization and dissociation. A larger fraction of molecules is dissipated through gas cooling mechanisms and thermal quenching. The synergy between ion mobility, dominated by convective flow, and the low SEI renders the production of free radicals per unit energy inefficient. This condition subsequently inhibits the molecular degradation rate [7, 12].

This phenomenon demonstrates that the production of RONS is highly dependent on the energy density available within the inter-electrode gap. At high SEI associated with low flow rates, gas molecules possess a prolonged residence time to interact with energetic electrons. The probability of excited species formation per unit power is rendered more optimal under these conditions [20]. The decline in EE at lower SEI and elevated flow rates indicated that a substantial portion of the energy was dissipated without inducing maximal molecular dissociation. This occurrence is attributed to the fact that the gas has exited the plasma zone prior to the reaction reaching a saturation point.

IV. CONCLUSIONS

This study successfully elucidates the fundamental correlation between the fluid dynamics of ambient air flow rates and the emission characteristics of reactive species, as well as the energy efficiency within a Dielectric Barrier Discharge (DBD) reactor. Characterization through Optical Emission Spectroscopy (OES) accurately demonstrates that the intensities of the primary active species, specifically hydroxyl radicals (OH), excited nitrogen (N2), and atomic oxygen (O), undergo significant reduction as the flow rate is increased from 2 LPM to 10 LPM.

This reduction in intensity is physically governed by ion mobility and the transition of the species transport regime. At low flow rates, the system is under kinetic control, wherein the electric field dominates ion movement, providing sufficient residence time for a high Specific Energy Input (SEI) accumulation to trigger maximum ionization.

ISSN No: -2456-2165 https://doi.org/10.38124/ijisrt/26mar2065

Conversely, at high flow rates, the dominance of convective transport causes the gas drag force to exceed the electrostatic force, which induces quenching phenomena and the dilution of electron density.

This condition exerts a direct impact on the Energy Efficiency (EE), wherein the utilization of input power is rendered most optimal under maximum SEI conditions at low flow rates. These findings provide a significant contribution to the development of DBD plasma technology in balancing intensive energy intake with gas flow control to maximize the production of reactive species for applications in the remediation of persistent pollutants.

ACKNOWLEDGMENT

This research was supported in part by Diponegoro University, Indonesia, through the RPI Research Funding Program (No. 569-126/UN7.D2/PP/V/2023). The authors would like to acknowledge the support provided by research assistants from the Plasma Research Center

REFERENCES

[1]. R. Garcia-Villalva, M. Biset-Peiro, A. Alarcon, S. Murcia-Lopez, and J. Guilera, “Catalytic bed configuration on the valorization of greenhouse gases by DBD,” vol. 525, no. October, p. 16815, 2025, doi: 10.1016/j.cej.2025.169815.

[2]. L. Li et al., “Carbon Capture Science & Technology Dielectric barrier discharge plasma catalysis for CO 2 conversion : Recent progress and perspectives,” Carbon Capture Sci. Technol., vol. 16, p. 100485, 2025, doi: 10.1016/j.ccst.2025.100485.

[3]. S. M. Pormazar et al., “Evolution and mechanistic enhancement of a novel dielectric barrier discharge plasma reactor for efficient dexamethasone degradation in aqueous solutions,” Chem. Eng. J., vol. 524, p. 169191, 2025.

[4]. K. Li et al., “Journal of Colloid And Interface Science Plasma catalytic ammonia synthesis in a fluidized-bed DBD reactor over M / Al 2 O 3 : Enhancement of plasma-catalyst surface interaction,” J. Colloid Interface Sci., vol. 683, no. P1, pp. 652–662, 2025, doi: 10.1016/j.jcis.2024.12.055.

[5]. D. Korzec et al., “Hybrid Dielectric Barrier Discharge Reactor : Production of Reactive Oxygen – Nitrogen Species in Humid Air,” Plama, vol. 8, pp. 1–28, 2025, doi: https://doi.org/10.3390/plasma8030027.

[6]. X. Yang, J. Li, and J. Cheng, “Effects of single and double dielectric barrier discharges on electric fields , discharge characteristics , reactive species , and microbial inactivation of food pathogens,” Food Res. Int., vol. 221, no. P1, p. 117307, 2025, doi: 10.1016/j.foodres.2025.117307.

[7]. C. Chen et al., “Degradation of micropollutants in secondary wastewater effluent using nonthermal plasma-based AOPs : The roles of free radicals and molecular oxidants,” Water Res., vol. 235, p. 119881, 2023, doi: 10.1016/j.watres.2023.119881.

[8]. H. Sulemana et al., “Synthesis and characterization of nickel ferrite (NiFe 2 O 4) nano-catalyst films for ciprofloxacin degradation,” Ceram. Int., vol. 51, no. 7, pp. 8376–8387, 2025, doi: 10.1016/j.ceramint.2024.12.268.

[9]. M. Hitzemann, C. Schaefer, A. T. Kirk, A. Nitschke, M. Lippmann, and S. Zimmermann, “Analytica Chimica Acta Easy to assemble dielectric barrier discharge plasma ionization source based on printed circuit boards,” Anal. Chim. Acta, vol. 1239, p. 340649, 2023, doi: 10.1016/j.aca.2022.340649.

[10]. C. Tian, N. Ahlmann, S. Brandt, J. Franzke, and G. Niu, “Optical characterization of miniature flexible micro-tube plasma (FμTP) ionization source A dielectric guided discharge,” 2021. doi: doi.org/10.1016/j.sab.2021.106222.

[11]. Y. Wang, Y. Chen, J. Harding, H. He, and A. Bogaerts, “Catalyst-free single-step plasma reforming of CH 4 and CO 2 to higher value oxygenates under ambient conditions,” Chem. Eng. J., vol. 450, no. P1, p. 137860, 2022, doi: 10.1016/j.cej.2022.137860.

[12]. C. Chen et al., “Degradation of perfluoroalkyl and polyfluoroalkyl substances (PFAS) in water by use of a nonthermal plasma-ozonation cascade reactor : Role of different processes and reactive species,” Chem. Eng. J., vol. 486, no. February, p. 150218, 2024, doi: 10.1016/j.cej.2024.150218.

[13]. Z. Xu et al., “Study on the effective removal of chlorpyrifos from water by dielectric barrier discharge (DBD) plasma : The influence of reactive species and different water components,” Chem. Eng. J., vol. 473, p. 144755, 2023, doi: https://doi.org/10.1016/j.cej.2023.144755.

[14]. B. Wang, J. Kong, and X. L. Key, “Preparation of MoO3γ-Al2O3 sulfur-resistant methanation catalyst with segmented plasma fluidized bed.pdf,” 2025. doi: https://doi.org/10.1016/j.cjche.2025.02.014.

[15]. J. Lou, H. Han, Z. Zhang, C. Feng, J. An, and X. Wang, “Citric acid modulated strong magnetic CoFe-LDH / CoFe 2 O 4 coupled dielectric barrier discharge plasma for efficient levofloxacin degradation : Enhanced internal electric field and accelerated electron migration,” J. Hazard. Mater., vol. 480, p. 136077, 2024, doi: 10.1016/j.jhazmat.2024.136077.

[16]. C. Oberste-Beulmann et al., “A SDBD Reactor for the Removal of Oxygen Traces in Hydrogen Operated above Atmospheric Pressure : Experiment and Simulation,” Plasma Chem. Plasma Process., vol. 45, pp. 1415–1430, 2025, doi: Awakowicz2,.

[17]. Y. Zhao, E. Hu, H. Ren, Z. Luo, G. Yin, and Z. Huang, “Modulating the dry reforming of CH 4 via non-thermal plasma under varied electrical waveforms,” J. Energy Inst., vol. 123, p. 102297, 2025, doi: 10.1016/j.joei.2025.102297.

[18]. D. Filice and S. Coulombe, “Observation and characterization of discharge mode transition in a three-electrode atmospheric pressure RF plasma system,” Plasma Sources Sci. Technol., vol. 34, no. 095015 (18pp), 2025, doi: https://doi.org/10.1088/1361-6595/ae05c7.

ISSN No: -2456-2165 https://doi.org/10.38124/ijisrt/26mar2065

[19]. C. Liu et al., “Based on size-exclusion effect of selective removal of organic pollutants in complex water quality by low temperature plasma : Degradation behavior and selective mechanism analysis,” Sep. Purif. Technol., vol. 354, p. 129252, 2025, doi: 10.1016/j.seppur.2024.129252.
[20]. Y. Xia et al., “Zn / Fe-MOF-Derived Carbon Nanofibers via Electrospinning for Efficient Plasma-Catalytic Antibiotic Removal,” catalysts, vol. 15, p. 944, 2025, doi: doi.org/10.3390/catal15100944.
[21]. N. Sunder, Y. Y. Fong, and S. L. S. Mun, “Preliminary Study on Syngas Production from a CO 2 and CH 4 Mixture via Non-Thermal Dielectric Barrier Discharge Plasma Incorporated with Metal – Organic Frameworks,” J. Compos. Sci., vol. 9, p. 148, 2025, doi: https://doi.org/10.3390/ jcs9040148.
[22]. Y. Liu, Z. Ning, M. Fang, X. Zhang, H. Guo, and M. An, “Rapid charge transfer and O 3 selective catalysis induced by B-doped nanoconfined reactor realized complete Cu-EDTA decomplexation : Significant role of BC 3 conformation,” Water Res., vol. 278, p. 123393, 2025, doi: 10.1016/j.watres.2025.123393.
[23]. D. P. Fuentes et al., “Plasma Diffuse Reflectance Infrared Fourier Transform Spectroscopy Cell Design and Experimental Set-Up for Operando-DRIFTS Investigations on Plasma-Induced Heterogeneous Catalyzed Reactions,” Chemistry—Methods, vol. 5, p. e202500057, 2025, doi: 10.1002/cmtd.202500057.
[24]. C. Vanlalhmingmawia, H. Moradi, Y. J. Kim, D. Kim, and J. Yang, “Synergy of nonthermal plasma and immobilized nanopillars-Ag (TiO 2) for the efficient degradation of antibiotics : Insight studies on plasma induced photocatalysis and degradation mechanism,” Chem. Eng. J., vol. 509, p. 161335, 2025, doi: 10.1016/j.cej.2025.161335.